Electronic Supplementary Material (ESI) for Energy & Environmental Science

The morphology-controlled synthesis of a nanoporous-antimony anode for high-performance sodium-ion batteries

Shuai Liu[a], Jinkui Feng*[a] , Xiufang Bian*[a], Jie Liu[b] and Hui Xu[a]

[a] *Key Laboratory for Liquid-Solid Structural Evolution and Processing of Materials (Ministry of Education), School of Materials Science and Engineering, Shandong University, Jinan 250061, China*

[b]*Advanced Fibers &Modern Textile Cultivation Base of State Key Lab, Qingdao University, Qingdao 266071, China*

Experimental Section

1. Material synthesis

$Al_{20}Sb_{80}$, $Al_{30}Sb_{70}$, $Al_{55}Sb_{45}$, $Al_{70}Sb_{30}$ and $Al_{90}Sb_{10}$ (at%) alloys were prepared from pure Al block (99.99 wt%) and pure Sb block (99.99 wt%). High-frequency induction heating was employed to melt the Al and Sb in a quartz crucible (at a temperature of 1200 °C for 5 min), and then the Al-Sb melt was cast into ingots in an iron chill mold. By using a single roller melt spinning apparatus (Model No. SP009A) (as shown in Fig.

*Corresponding author.
E-mail address: jinkui@sdu.edu.cn (J. K. Feng); xfbian@sdu.edu.cn (X.F. Bian)

S2), the Al-Sb ingots were remelted in a quartz tube by high-frequency induction heating and melt-spun onto a copper roller at a circumferential speed of about 27 m s^{-1}. The Al-Sb ribbons obtained were typically 30-50 μm in thickness, 2-5 mm in width, and several centimeters in length. The dealloying of the melt-spun Al-Sb ribbons was performed in a 20 wt% NaOH aqueous solution with water bath at 60 °C for 12 h. The magnetic stirring (Model No. JJ-I) was at a rate of 600 r/min. Abundant gas bubbles generated on the surface of the ribbons at the beginning of the dealloying reaction which finished when no bubbles emerged in the NaOH solution. After dealloying, the precipitation was filtered with filter paper and rinsed with distilled water for several times, followed by drying for 24 h at 80 °C under vacuum. The as-prepared samples were kept in a vacuum chamber to avoid oxidation.

2. Sample Characterization

The microstructure of the as-prepared materials were characterized by scanning emission microscope (SEM, HITACHI SU-70), high resolution transmission electron microscope (HRTEM, JEOL JEM-2100). The structure was characterized using X-ray diffraction (XRD, Rigaku Dmax-rc diffractometer) and LabRAM HR800 spectrometer for Raman spectra. The specific surface area, porosity (V_{pore}), and pore-size distribution were analyzed using a mercury porosimeter (AutoPore IV 9500).

3. Electrochemical Measurements

The as-prepared active material or commercial Sb powder (several micrometers, Aladdin Industrial Co., Ltd.) was mixed with super P (purchased from lzy battery sales department in China) and a carboxymethyl cellulose (CMC) binder (70 : 15 : 15 in weight) in deionized water to form a homogenous slurry, which was painted on a copper foil (purchased from lzy battery sales department in China) and then dried at 100 °C under vacuum for 12 h to form the electrodes. Na sheet (home-made) was used as the counter electrode, and Celgard 2400 was used as the separator. The electrolyte was a mixture of 1 M $NaClO_4$ in propylene carbonate with 5% fluoroethylene carbonate (FEC) additive. All the cells (CR2016 coin-type) (purchased from lzy battery sales department in China) were assembled in a glove box with water/oxygen content lower than 1 ppm and tested at room temperature. Cyclic voltammetric measurements were carried out with the coin cells at a scan rate of 0.1 mv s^{-1} between 0.1 V and 2.0 V (vs. Na^+/Na) using a CHI 660E electrochemical workstation (Shanghai, China). Galvanostatic discharge/charge cycles were performed between 0.1 and 1.5 V (vs. Na^+/Na) on a Neware-CT-3008 test system (Shenzhen, China). Electrochemical impedance spectroscopy (EIS) was also performed on a CHI 660E electrochemical workstation with a frequency of 100 kHz to 0.01 Hz.

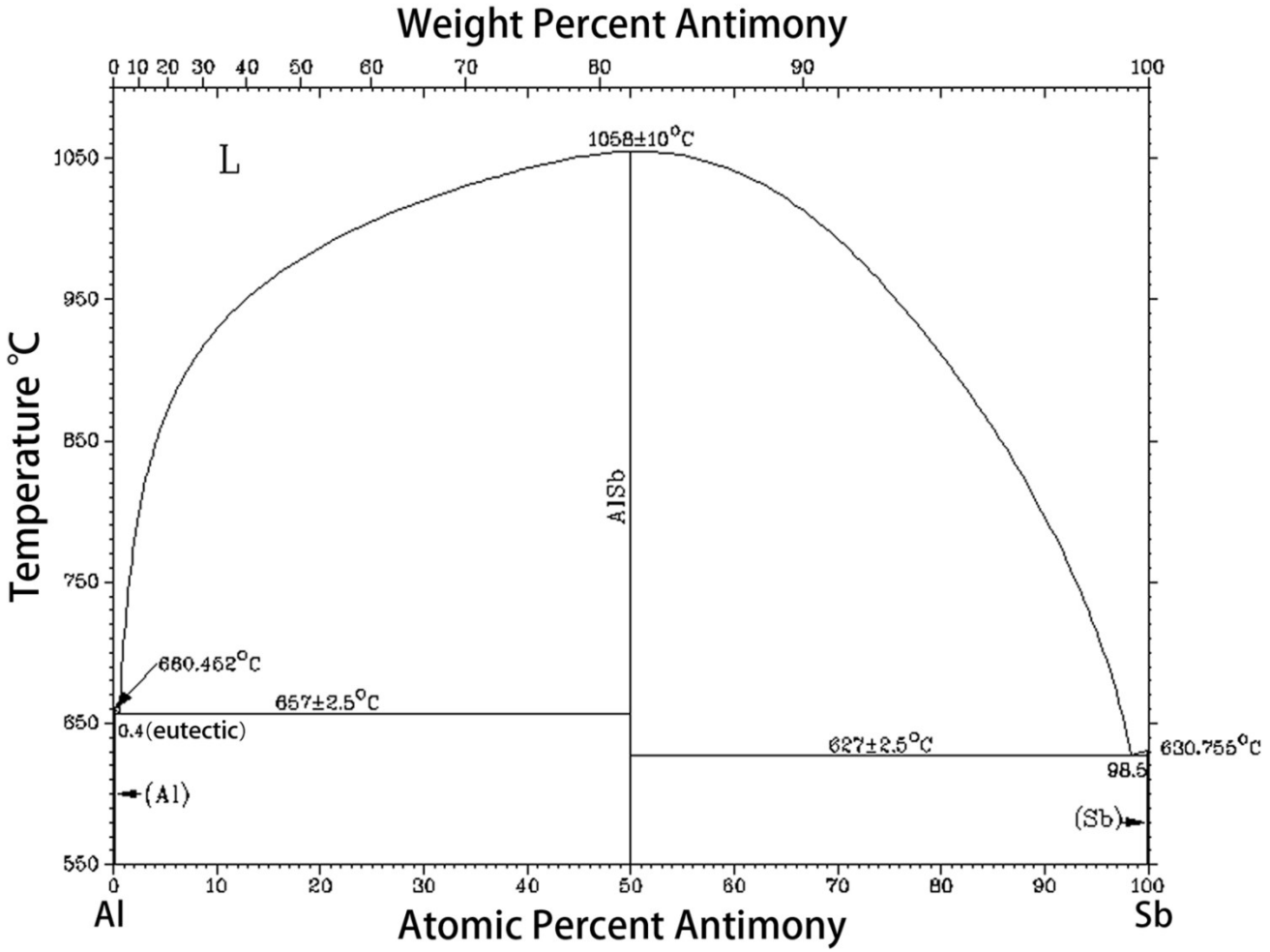

Fig. S1. Al-Sb phase diagram [1, 2]

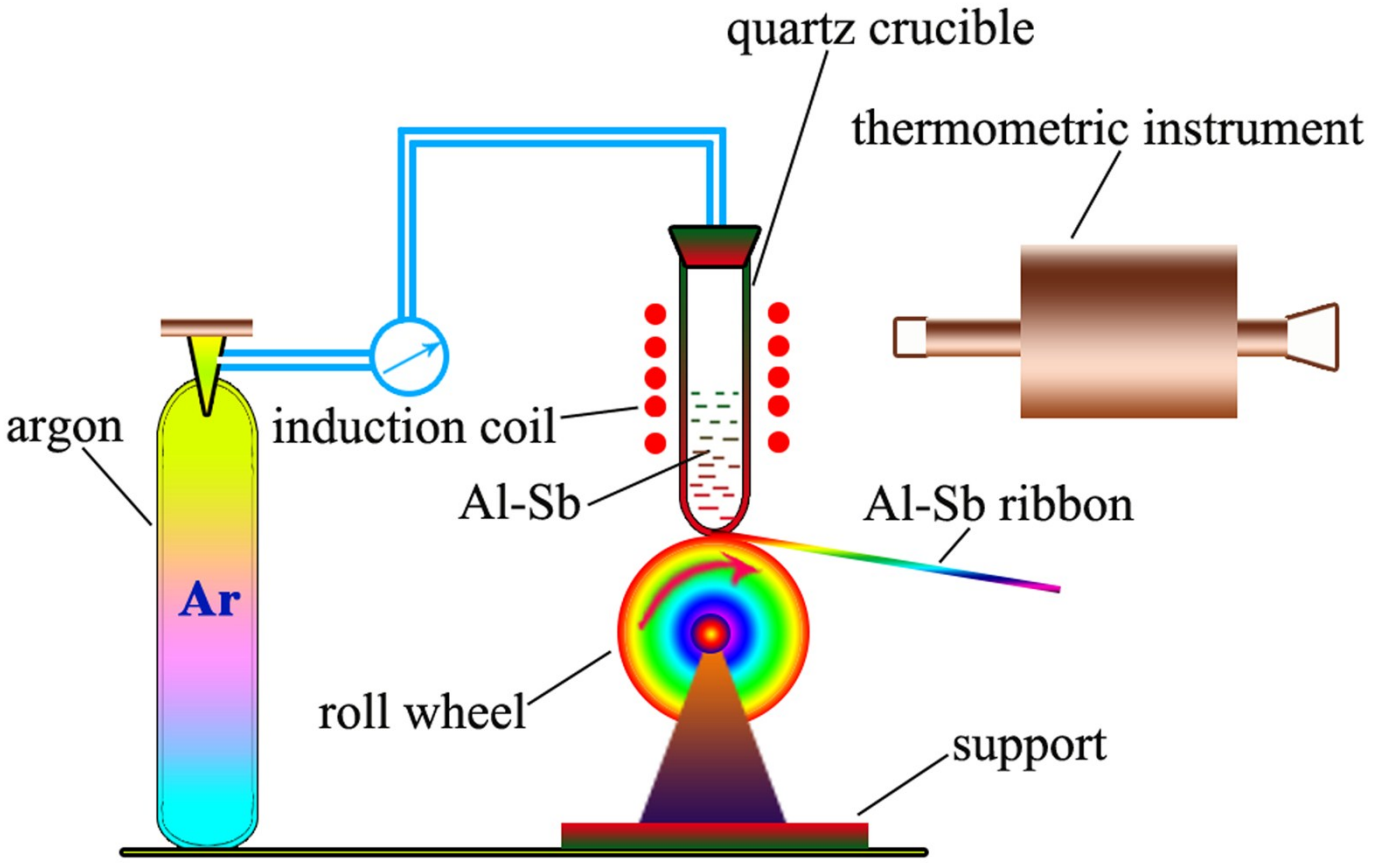

Figure S2. Schematic diagram of single roller melt spinning apparatus

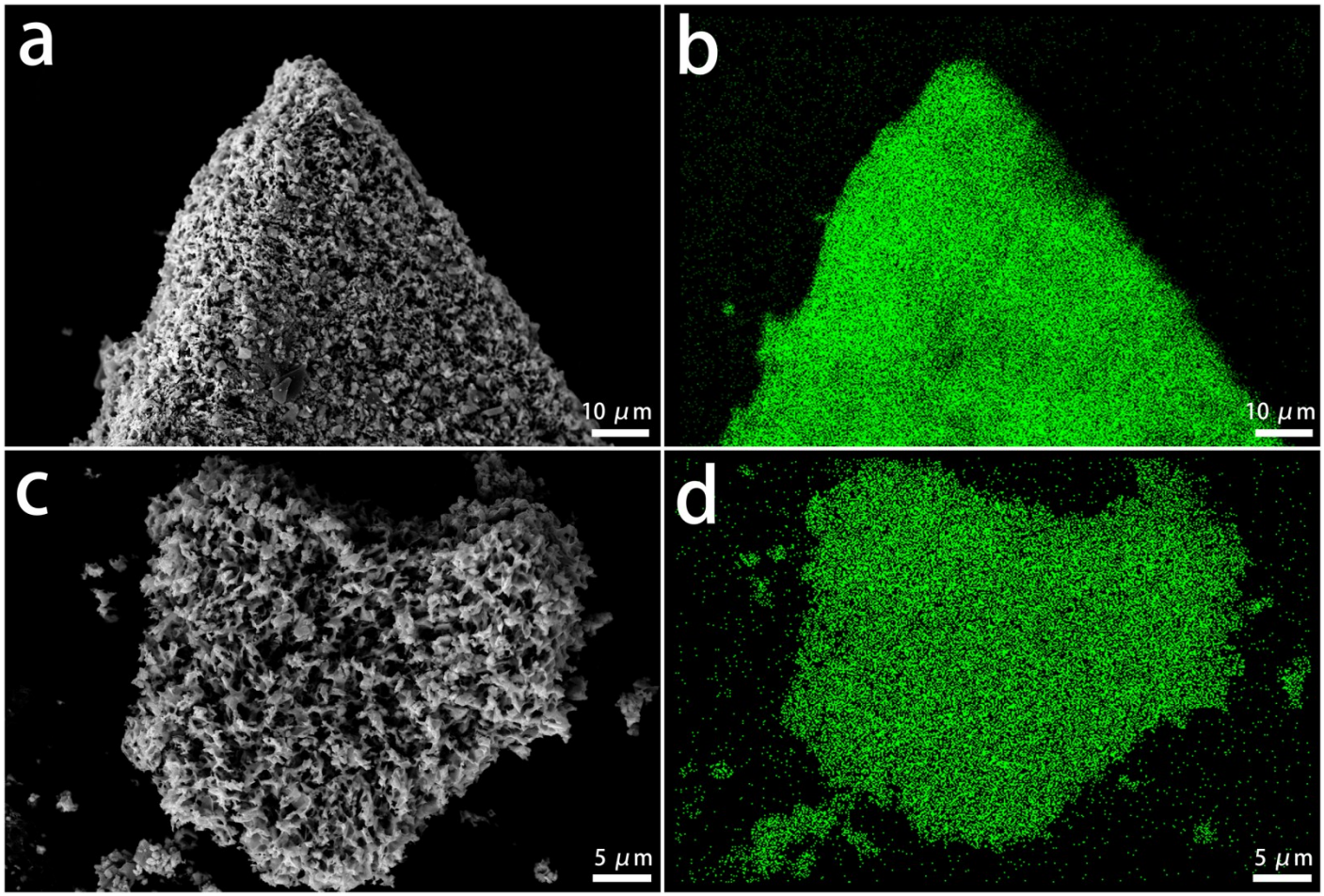

Fig. S3. (a) SEM image of coral-like NP-Sb70. (b) EDX mapping of elemental Sb corresponding to (a). (c) SEM image of honeycomb-like NP-Sb80. (d) EDX mapping of elemental Sb corresponding to (c)

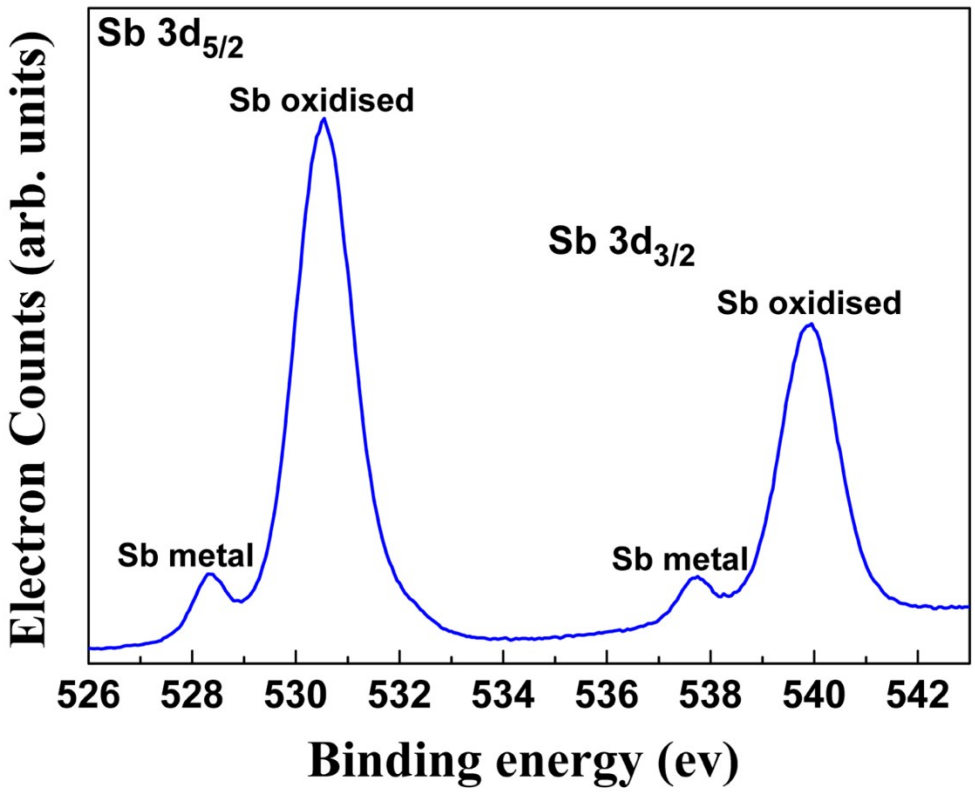

Fig. S4. Sb 3d XPS spectrum measured from the surface of the NP-Sb70 powder exposed to air for 24 h. The peak energies (Sb metal and Sb oxidised) are close to the binding energies reported for Sb 3d in metal and oxides.[3-5]

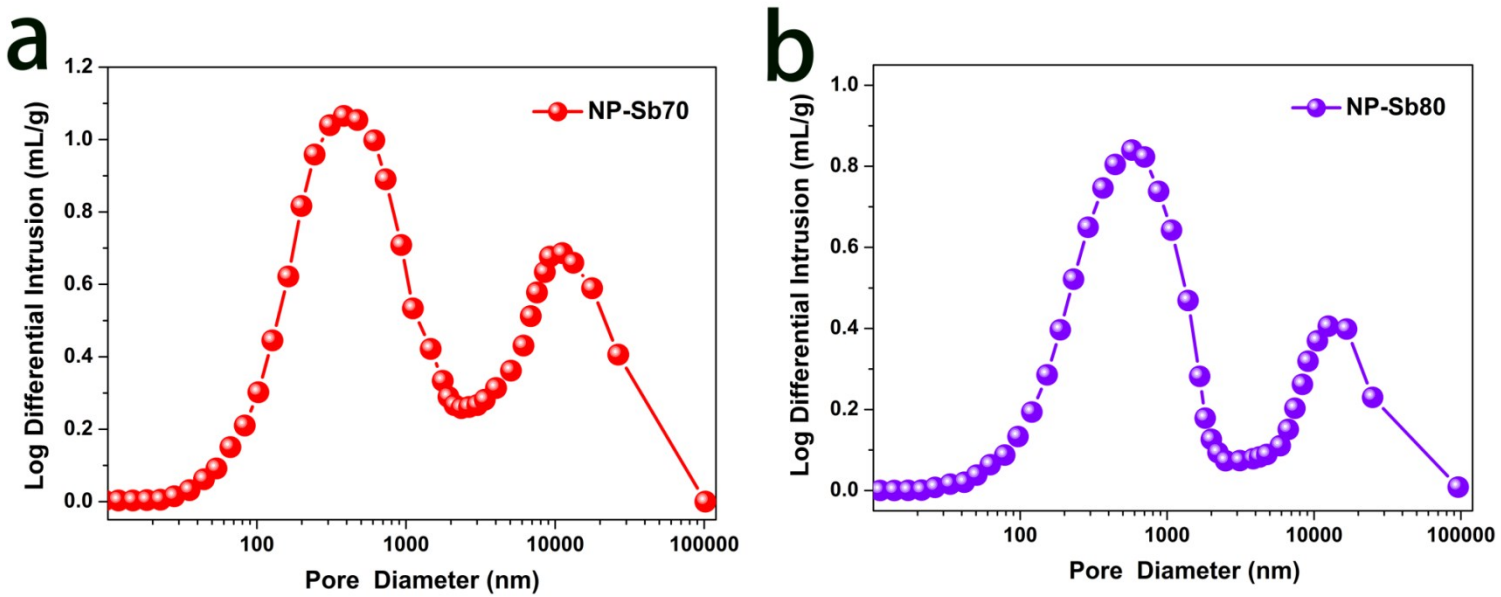

Fig. S5. Pore-size distribution in the NP-Sb70 (a) and NP-Sb80 (b), measured by mercury porosimetry.

In Fig. S5a and Fig. S5b the first peak (in the region of small pore size) represents intragrain nanopores, while another peak at larger pore size represents intergrain macropores, which we generally observed in the powder sample. The average nanopore size, porosity (V_{pore}), and specific surface area of the NP-Sb70 are 385.1 nm, 69.2% and 11.7 m^2/g, respectively. The average nanopore size, porosity (V_{pore}), and specific surface area of the NP-Sb80 are 576.9 nm, 50.4% and 6.3 m^2/g, respectively. The V_{pore} and specific surface area of the NP-Sb70 are larger than those of the NP-Sb80.

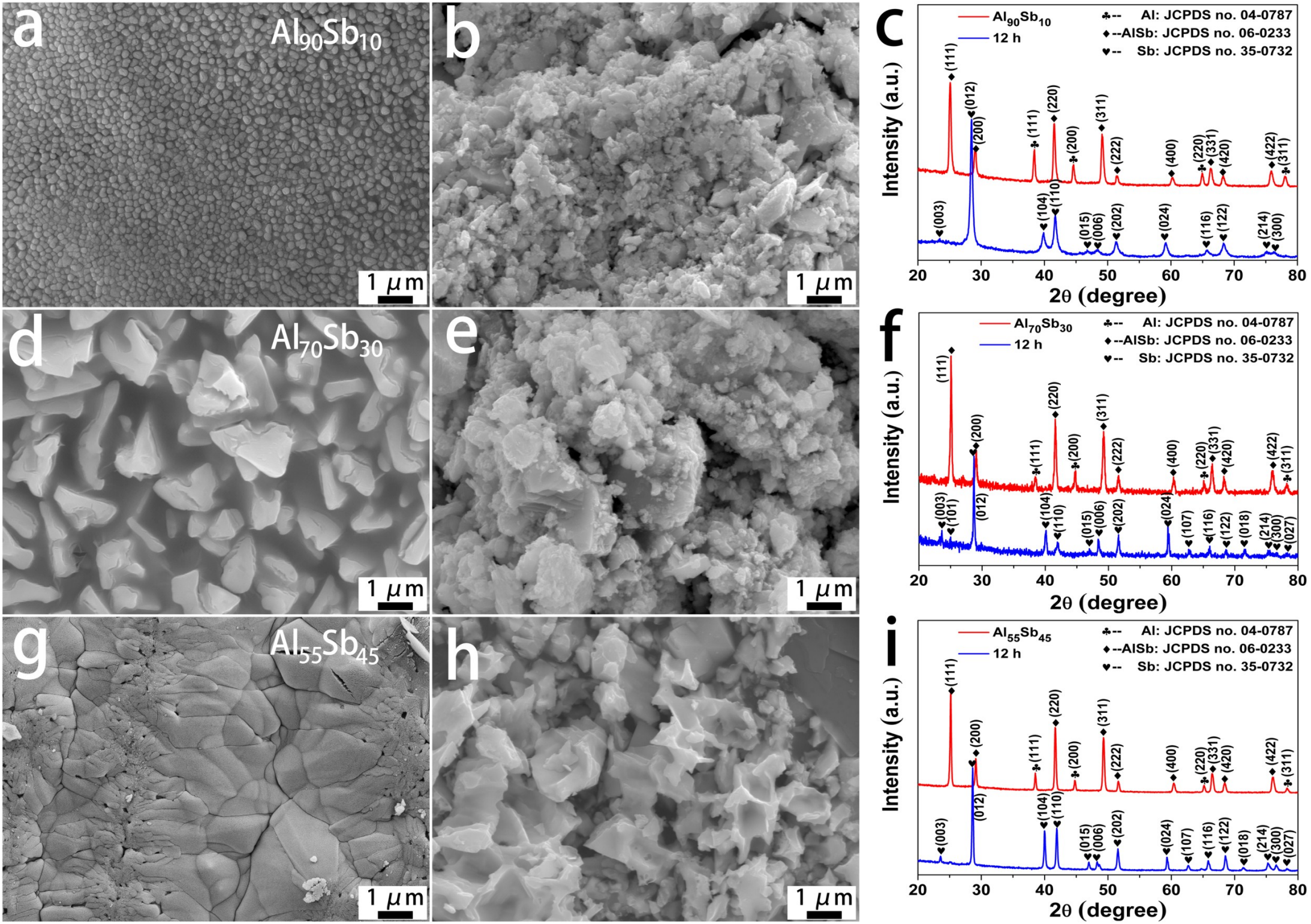
a
$Al_{90}Sb_{10}$
1 μm
b
1 μm
c
$Al_{90}Sb_{10}$
12 h
♣-- Al: JCPDS no. 04-0787
♦--AlSb: JCPDS no. 06-0233
♥-- Sb: JCPDS no. 35-0732
Intensity (a.u.)
2θ (degree)
d
$Al_{70}Sb_{30}$
1 μm
e
1 μm
f
$Al_{70}Sb_{30}$
12 h
♣-- Al: JCPDS no. 04-0787
♦--AlSb: JCPDS no. 06-0233
♥-- Sb: JCPDS no. 35-0732
Intensity (a.u.)
2θ (degree)
g
$Al_{55}Sb_{45}$
1 μm
h
1 μm
i
$Al_{55}Sb_{45}$
12 h
♣-- Al: JCPDS no. 04-0787
♦--AlSb: JCPDS no. 06-0233
♥-- Sb: JCPDS no. 35-0732
Intensity (a.u.)
2θ (degree)

Fig. S6. (a) SEM image of $Al_{90}Sb_{10}$ alloy ribbon. (b) SEM image of Sb10 ($Al_{90}Sb_{10}$ immersed in the 20wt% NaOH aqueous solution at 60 °C for 12 h) (c) XRD patterns of $Al_{90}Sb_{10}$ alloy ribbon and Sb10. (d) SEM image of $Al_{70}Sb_{30}$ alloy ribbon. (e) SEM image of Sb30 ($Al_{70}Sb_{30}$ immersed in the 20wt% NaOH aqueous solution at 60 °C for 12 h). (f) XRD patterns of $Al_{70}Sb_{30}$ alloy ribbon and Sb30. (g) SEM image of $Al_{55}Sb_{45}$ alloy ribbon. (h) SEM image of Sb45 ($Al_{55}Sb_{45}$ immersed in the 20wt% NaOH aqueous solution at 60 °C for 12 h). (i) XRD patterns of $Al_{55}Sb_{45}$ alloy ribbon and Sb45.

Fig. S6a shows an SEM image of as-prepared $Al_{90}Sb_{10}$ alloy ribbon precursor. The XRD pattern in Fig. S6c shows the formation of simple substance Al (JCPDS no. 04-0787) and intermetallic compound AlSb (JCPDS no. 06-0233) in the $Al_{90}Sb_{10}$ alloy ribbon. Fig. S6b shows an SEM image of Sb10 (Al90Sb10 immersed in the 20wt% NaOH aqueous solution at 60 °C for 12 h). The XRD pattern in Fig. S6c (12h) exhibits that Al is etched away to form the Sb particle (Sb10), containing no Al. The structural evolutions of the Sb30 (as shown in Fig. S6d-f) and Sb45 (as shown in Fig. S6g-i) are similar to the Sb10. The particle size order is Sb10 (Fig.S6b) < Sb30 (Fig. S6e) < Sb45 (Fig. S6h).

References

1. C. A. Coughanowr, U. R. Kattner and T. J. Anderson, *Calphad*, 1990, **14**, 193-202.

2. K. Yamaguchi, K. Itagaki and Y. Chang, *Calphad*, 1996, **20**, 439-446.

3. M. D. Allen, S. Poulston, E. G. Bithell, M. J. Goringe and M. Bowker, *J Catal*, 1996, **163**, 204-214.

4. F. Montilla, E. Morallón, A. De Battisti, S. Barison, S. Daolio and J. L. Vázquez, *The Journal of Physical Chemistry B*, 2004, **108**, 15976-15981.

5. F. Garbassi, *Surf Interface Anal*, 1980, **2**, 165-169.